Published in final edited form as:
*Adv Energy Mater*. 2019 February 7; 9(6): . doi:10.1002/aenm.201803096.

# Highly Solvating Electrolytes for Lithium-Sulfur Batteries

**Abhay Gupta**, **Amruth Bhargav**, **Arumugam Manthiram**
Materials Science and Engineering Program & Texas Materials Institute, The University of Texas at Austin, Austin, TX 78712, USA

## Abstract

There is a critical need to evaluate lithium-sulfur (Li-S) batteries with practically relevant high sulfur loadings and minimal electrolyte. Under such conditions, the concentration of soluble polysulfide intermediates in the electrolyte drastically increases, which can alter the fundamental nature of the solution-mediated discharge and thereby the total sulfur utilization. In this work, we present an investigation into various high donor number (DN) electrolytes that allow for increased polysulfide dissolution, and demonstrate how this property may in fact be necessary for increasing sulfur utilization at low electrolyte and high loading conditions. The solvents dimethylacetamide, dimethyl sulfoxide, and 1-methylimidazole are holistically evaluated against dimethoxyethane as electrolyte co-solvents in Li-S cells, and they are used to investigate chemical and electrochemical properties of polysulfide species at both dilute and practically relevant conditions. The nature of speciation exhibited by lithium polysulfides is found to vary significantly between these concentrations, particularly in regards to the $S_3^{\bullet-}$ species. Furthermore, the extent of the instability in conventional electrolyte solvents and high DN solvents with both lithium metal and polysulfides is thoroughly investigated. These studies establish a basis for future efforts into rationally designing an optimal electrolyte for a lean electrolyte, high energy density Li-S battery.

### Keywords

lithium-sulfur batteries; polysulfide speciation; UV-vis spectroscopy; high concentration; donor number

## 1. Introduction

The advent of lithium-ion batteries has enabled tremendous societal advancement in terms of electrically enabled phones, laptops, and other devices, and situates society on the cusp of future technological leaps in electric vehicles and large-scale grid storage. These future advances will necessitate battery chemistries with significantly higher energy density than that of the current state-of-the-art lithium-ion batteries. The lithium-sulfur (Li-S) battery chemistry has proven to be a promising alternative. Sulfur cathodes have a high theoretical capacity of 1,672 mA h $g^{-1}$, nearly 10 times that of insertion cathodes.[1-3] As opposed to traditional systems, the discharge of sulfur results in the formation of various redox-active

manth@austin.utexas.edu (A. Manthiram).

Supporting Information
Supporting Information is available from the Wiley Online Library or from the author.

lithium polysulfide ($Li_2S_x$, $2 < \times \leq 8$) intermediates that are soluble in the electrolyte solvent. In such a system, the close interplay between the soluble active material and solvent amplifies the importance of understanding the complex speciation and disproportionation exhibited by polysulfide species. Investigating the impact of minimized electrolyte on the chemical environment surrounding the cathode and solution-mediated discharge pathways is crucial for optimizing the performance.

In practice, the large theoretical capacity of sulfur cathodes cannot be fully utilized, particularly at high loadings of sulfur, low electrolyte amounts, or kinetically limiting low temperatures.[2,4] Sulfur and its lithium sulfide ($Li_2S$) discharge product are highly insulating and present significant barriers towards electron flow and subsequent electrochemical reactions.[3] However, the Li-S chemistry can overcome the limitations of the insulating surface-based pathways through polysulfide-assisted solution-based reaction pathways, which can allow for moderate utilization. The solution-based pathway involves an initial reduction of sulfur at the triple-phase-boundary of the conductive cathode carbon substrate, the solid sulfur particle, and the electrolyte.[5] The solid species reduces to intermediate lithium polysulfide species, which proceeds to dissolve, dissociate, and disproportionate into a vast array of different chain-length polysulfides in the liquid electrolyte. Upon saturation, further reduction of polysulfides must proceed through a surface-based reaction pathway to nucleate solid-state $Li_2S$ onto the cathode substrate. The initial solution-based reduction pathway is quite fast and kinetically favorable because lithium polysulfides can enable facile charge transfer in solution.[6] This nature has even prompted their use in numerous studies as an electrolyte additive.[7-10] In comparison, the subsequent surface-based reduction can be kinetically unfavorable given the highly insulating nature of $Li_2S$, which passivates the cathode and can block further reduction.[11] Due to this, a significant amount of unutilized sulfur and polysulfide species can remain after a sulfur cathode completes discharging and the cell reaches its lower voltage limits.[1,11]

The limitations posed by the surface-based reaction pathways in Li-S batteries beckon further investigation into the solution-mediated discharge behavior at practically relevant conditions. Furthermore, there is a critical need to investigate alternative electrolyte solvents that can augment and extend the duration of the advantageous solution-mediated discharge. With such modifications, fundamentally new and alternative strategies that consider increasing the overall solubility of polysulfide intermediates can be explored, tuning the Li-S discharge behavior for instrumentally greater utilization.

## 2. Results and Discussion

### 2.1. Need for High Polysulfide Solubility:

The predominantly used electrolyte solvent in the Li-S literature consists of 1:1, by volume, 1,2-Dimethoxyethane (DME) and 1,3-Dioxolane (DOL) solvents.[1] At room temperature, this electrolyte formulation exhibits a maximum solubility of approximately 6 M to sulfur species in the form of soluble polysulfides, or expressed in another way, 1 M of $Li_2S_6$; this serves as a ceiling for the amount of polysulfide species that can dissolve into solution during the facile solution-based stage of discharge.[11] As such, having large amounts of

electrolyte in a cell and low loadings of sulfur on the cathode side can accommodate for relatively larger amounts of polysulfide species to dissolve into the electrolyte solution. It is for this reason that cells made with high electrolyte amounts and low sulfur loadings typically have higher attained specific capacities with respect to active material in the cathode, but lower overall energy density.[3,12] Using low electrolyte amounts in Li-S cells generally leads to significantly lower attained specific capacities, as well as rapid consumption of what little electrolyte there is by the reactive lithium-metal anode.[13]

The success of Li-S chemistry is dependent on its ability to outperform traditional lithium-ion batteries. The achievable specific energy of the Li-S battery is uniquely dependent on the interplay between dissolved polysulfide species and the electrolyte-to-sulfur (E/S) ratio (in $\mu L_{electrolyte}\ mg^{-1}{}_{sulfur}$). This functional relationship has been calculated here at a cell level assuming a sulfur cathode with 75% sulfur content at various sulfur loadings along with a perfectly matched lithium anode (please see supplemental information for details). Figure 1a illustrates this interplay for a “theoretical” system employing 100% sulfur utilization (1,672 mA h $g^{-1}$) while Figure 1b assumes a more commonly observed “practical” utilization of nearly 60% (1,000 mA h $g^{-1}$).

In the theoretical case, E/S ratios of 5 μL $mg^{-1}$ or lower are necessary to achieve a specific energy of at least 500 W h $kg^{-1}$, which serves as a pervasive target in the research community for Li-S batteries.[3,12,14] This E/S ratio corresponds to a concentration of approximately 1 M $Li_2S_6$ (or 6 M of sulfur) that would have to be dissolved into the electrolyte during the course of discharge. At more practical sulfur utilization, the required E/S ratio to achieve this specific energy would be 2 μL $mg^{-1}$ or lower. This corresponds to a $Li_2S_6$ concentration of 1.6 M (or 9.6 M of sulfur) that would have to dissolve into the electrolyte during discharge.

In both of these scenarios, the amount of sulfur required to be dissolved in solution to have completely facile solution-based discharge approaches and exceeds the theoretical maximum polysulfide solubility in DOL-DME at room temperature. Clearly, this is a contributing factor to the difficulty in achieving high specific capacities when discharging Li-S cells with high sulfur loadings and low E/S ratios.[12] This enforces the need to investigate electrolyte solvents with increased solubility towards polysulfide species and evaluate their potential as an alternative strategy for increasing utilization of sulfur.

Many approaches in the literature have demonstrated the opposite approach of impeding the dissolution of intermediate polysulfide species through sparingly soluble electrolytes.[15-17] Doing so can improve Li-S cyclability, as they minimize the shuttling and loss of active material over the course of cycling. However, limiting solvation of polysulfide intermediates requires greater reliance on surface-dependent conduction pathways, which can be quite insulating and kinetically limiting in comparison. This issue can be circumvented by employing low areal loadings of sulfur in the cathode (~ 1 to 2 mg $cm^{-2}$), but this presents a penalty to cell level energy density. On the other hand, a highly solvating electrolyte may yield great benefits to sulfur utilization at high areal sulfur loadings but would also present challenges to long-term cycling due to increased polysulfide shuttling. For practical implementation in the future, such a strategy would likely require the use of a passivating

lithium metal protection layer that could prevent the reaction of shuttling soluble polysulfides with the lithium-metal anode. Nonetheless, the highly solvating strategy merits further investigation as a contender in enabling practical, energy-dense Li-S batteries.

### 2.2. Solubility and Speciation:

While a solvent such as DME offers a solubility to polysulfide species of 1 M $Li_2S_6$, high donor number (DN) solvents such as N,N-dimethylacetamide (DMA), dimethyl sulfoxide (DMSO), and 1-methylimidazole (MeIm) could have the potential to offer enhanced solubility. These solvents represent a broad range of donor numbers and dielectric constants (shown in Figure 2a) and have been explored in previous electrochemical studies with both Li-S as well as Li-$O_2$ systems on a fundamental basis.[5,18-21] However, the electrochemistry in these solvents at high polysulfide concentrations, reflective of practical high sulfur loadings and low E/S ratios, has not previously been investigated. The possible use of such solvents in the liquid electrolyte of lithium-sulfur batteries is compelling when formulating a strategy to enhance sulfur utilization at practically relevant conditions. As such, these high donor number solvents were selected as standards with which to investigate this strategy in more detail.

As mentioned previously, a $Li_2S_6$ solubility of 1.6 M is required to unlock the desired high specific capacities in Li-S cells, but DOL-DME is incapable of delivering this solubility at room temperature. As shown in Figure 2a, DOL-DME is unable to dissolve a concentration of 1.5 M $Li_2S_6$ species, a clear sign that the solution is past its saturation point. On the other hand, the high donor number solvents DMA, DMSO, and MeIm are very capable of accommodating such high polysulfide concentrations, showing complete dissolution of 1.5 M $Li_2S_6$ at room temperature. Though each sample contains lithium and sulfur in a mole ratio equivalent to $Li_2S_6$, the polysulfide species clearly disproportionate and dissociate into a broad continuum of polysulfide species, as evident by the vials containing a low concentration of 0.1 mM "$Li_2S_6$" in Figure 2a. The clear blue color present in vials containing DMA and DMSO reveals the presence of the $S_3^{\bullet-}$ species.[5,22] This radical species is stabilized by the increased donicity of high DN solvents and can function as a redox mediator in solution. It can allow for charge transfer and reduction to occur in the bulk of the electrolyte, alleviating the need for reduction to occur at explicit triple-phase interfaces.[5,19,23,24]

A fundamental understanding of each solvent's lithium polysulfide speciation at high concentrations is critical to systematically designing an enhanced electrolyte, as this is a major indicator of the predominant reaction pathways during sulfur reduction. Extensive *in-situ*, in-operando, and *ex-situ* absorbance studies have been performed in the past on polysulfide speciation in a variety of solvents, but these studies have exclusively been performed at low concentrations ranging from 0.016 to 0.1 M of sulfur.[19,23,25-27] While such studies are interesting from a fundamental perspective, high concentration absorbance studies must be performed in order to gain a realistic understanding of the polysulfide speciation that occurs in a practical, energy dense, lean electrolyte Li-S battery.[12] Higher concentration absorbance studies are difficult to perform due to the intrinsic limitations in the opacity of polysulfide solutions (which proceed to saturate the detector of most

instruments), but this can be overcome by using short-path-length cuvettes. In this study, 0.01 mm path-length cuvettes enabled the use of ultraviolet-visible (UV-Vis) spectrophotometry to characterize polysulfide speciation at high concentrations of 0.25 M nominal $Li_2S_6$ (1.5 M of sulfur). This concentration was the maximum achievable without saturating the instrument's detector and likely tends towards the speciation encountered in practical Li-S cells.

As seen in Figure 2b, DMA exhibits by far the largest relative amount of the $S_3^{\bullet-}$radical species at 618 nm, with 5 times the relative concentration of that found in DMSO and MeIm, while DOL-DME exhibits no discernable peak. DMSO and MeIm exhibit the largest relative intensities for $S_6^{2-}$ species, with peaks at 350 and 475 nm showing values of 10-30% higher than that for DMA, while again, DOL-DME exhibits no peaks for this speciation. In fact, DOL-DME seems to exhibit preferential speciation to $S_4^{2-}$, with greater peak intensities at 300 and 420 nm, matching what is observed at lower concentrations (Figure S1).[19] However, the high concentration spectra for the high DN solvents substantially differ from what is observed for them at low concentrations. At high concentration, all of the high DN solvents exhibit increased relative presence of $S_6^{2-}$and reduced presence of $S_3^{\bullet-}$, indicating that the equilibrium tends to shift towards $S_6^{2-}$ speciation at high concentration. The $S_6^{2-}$ peaks at 475 nm show intensities almost 6 times larger than that of $S_3^{\bullet-}$ in DMSO and MeIm, while they exhibit roughly equal intensities in DMA. This suggests that the exact reduction pathway may differ at high concentrations from what has been reported in the past. Elemental sulfur is reduced (Equation 1) in a two electron process, after which it disproportionates and rapidly dissociates to $S_6^{2-}$ and $S_3^{\bullet-}$, respectively (Equations 2 and 3).

$$S_8 + 2e^- \rightarrow S_8^{2-} \tag{1}$$

$$S_8^{2-} \rightarrow S_6^{2-} + 1/4S_8 \tag{2}$$

$$S_6^{2-} \rightarrow 2S_3^{\bullet-} \tag{3}$$

Polysulfide species are then further reduced to lower order polysulfides, with the $S_3^{\bullet-}$ radical playing a key intermediate role in these reactions (Equations 4, 5, and 6) before ultimately being reduced to solid state $Li_2S$. $S_8^{2-}$ is reduced in Equation 6 in parallel to the disproportionation occurring in Equation 2.[5,19]

$$S_3^{\bullet-} + e^- \rightarrow S_3^{2-} \tag{4}$$

$$2S_3^{\bullet-} + 2S_3^{2-} \rightarrow 2S_4^{2-} \tag{5}$$

$$S_8^{2-} + 2e^- \rightarrow 2S_4^{2-} \tag{6}$$

This reaction pathway depends heavily on the rapid $S_3^{\bullet-}$ dissociation in Equation 3, and this may still be the case for DMA at high concentrations due to the substantial presence of $S_3^{\bullet-}$. However, this dissociation does not seem to be as rapid in DMSO and MeIm at high concentrations, as the considerable presence of $S_6^{2-}$ compared to the $S_3^{\bullet-}$ species suggests that the equilibrium shifts significantly to the left in Equation 3. This is interesting when considering the use of these solvents in a lean electrolyte Li-S battery, as while the $S_3^{\bullet-}$ radical species may have a presence during discharge of sulfur in these solvents, its exact role may significantly differ from what is reported in the reaction mechanism at low concentrations. It may play a role as a temporary reaction intermediate, driving further reduction through alternative pathways, but never remain as a lasting dominant species at any point during discharge. The speciation represented here merely represents a snapshot during the entire discharge route, and further *in-situ* and *in-operando* studies at high concentration will be needed to evaluate this hypothesis and investigate speciation across the entire range of discharge. Strong presence of the $S_3^{\bullet-}$ species at high concentration also does not seem to be directly correlated to either donor number or dielectric constant, which may indicate the need for another metric in describing the preferential stabilization of radical species.

### 2.3. Electrochemical Utilization:

The ability of these solvents to have tangible effects on the electrochemical utilization of a sulfur cathode was further assessed through galvanostatic discharge of Li-S cells. Sulfur cathodes with an areal loading of 2 mg $cm^{-2}$ (E/S = 20 μL $mg^{-1}$) were used to assess the utilization behavior in these solvents, followed by higher loading tests at 6 mg $cm^{-2}$ (E/S = 10 μL $mg^{-1}$). The deliberate variation in areal loading and E/S parameters allowed for assessment of utilization in each solvent at both dilute and concentrated polysulfide conditions. This is particularly useful for investigating how the nature of solution-mediated discharge deviates from ample electrolyte conditions to practical low-electrolyte amounts. Each solvent was used in an electrolyte with 50% DOL and 1 M Lithium bis(trifluoromethanesulfonyl)imide (LiTFSI) as a direct comparison to the predominantly used DOL-DME electrolyte formulation. In DOL-DME electrolyte, DOL acts to help stabilize lithium metal while DME operates as the primary solvating agent of lithium polysulfide species, so this format was replicated for the high DN solvents being investigated.[28,29]

As shown in Figure 3a **and** b, cells containing DMA and DMSO exhibit a clear increase in initial capacity by about 10% compared to those with DME, attaining average capacities of around 1,250 mA h $g^{-1}$ compared to 1,100 mA h $g^{-1}$ in DME. Similar trends are seen for cells containing DMA at high sulfur loadings shown in Figure 3c **and** d, exhibiting an average initial capacity of 670 mA h $g^{-1}$ compared to 540 mA h $g^{-1}$ in DME, an increase of 24%. This strongly suggests that the ability to dissolve greater amounts of polysulfide species and presence of the $S_3^{\bullet-}$ species has a beneficial effect on increasing sulfur utilization. Interestingly, while cells containing DMSO solvent at low sulfur loadings exhibit utilization similar to DMA, this behavior subsides at high loading, where cells with DMSO only exhibited average initial capacities of 570 m Ah $g^{-1}$. This strongly corroborates the speciation data uncovered through the previous UV-Vis study; presence of $S_3^{\bullet-}$ in DMSO

diminishes at the high concentrations encountered in high loading, lean electrolyte cells seen here, which has a palpable effect on the observed utilization. Additionally, the high loading voltage profile in DOL-DMA electrolyte exhibits a large nucleation overpotential followed by recovery of voltage between 250 and 700 mA h $g^{-1}$, which is attributed to the greater presence of $S_3^{\bullet-}$, driving further precipitation of $Li_2S$ compared to that in the other electrolytes.

Cells containing electrolyte made with MeIm solvent had low initial capacities of 150 mA h $g^{-1}$ at 2 mg $cm^{-2}$ and 470 mA h $g^{-1}$ at 6 mg $cm^{-2}$, indicating largely irreversible side reactions may be occurring between the solvent and electrode during discharge. Additionally, large second plateau overpotentials of as high as 100 mV and 400 mV, respectively, in the 2 mg $cm^{-2}$ and 6 mg $cm^{-2}$ cells are even further indicative of significant instability with the lithium-metal anode. This is further supported by visual inspection of anodes retrieved after the first cycle (Figure S2). The instability with lithium metal may be masking the already substantial utilization observed in DOL-DMA due to the abundant $S_3^{\bullet-}$ species, preventing this electrolyte from achieving its full potential.

### 2.4. Stability Studies:

As these solvents exhibit signs of instability with lithium metal over the course of discharge, there is a critical need to understand the magnitude and mechanism behind this instability for each solvent.[5,18] As such, the long-term stability of these solvents in contact with lithium metal was thoroughly investigated. Lithium symmetric cells were constructed with electrolytes containing 1 M LiTFSI in DOL-DME, DOL-DMA, DOL-DMSO, and DOL-MeIm solvents in order to isolate and evaluate the electrochemical stability of each solvent in contact with lithium metal, shown in Figure 4.

As shown in Figure 4a, cells containing DMA and MeIm fail rapidly upon the application of current. Cells with DMSO were capable of cycling, but with drastically high and variable overpotentials of 150 mV, indicating clear instability with lithium metal. On the other hand, cells containing DOL-DME perform much better, with low, consistent overpotentials on the order of 50 mV. After one lithium plating and stripping cycle, electrochemical impedance spectroscopy was performed to corroborate the symmetric cell data with the impedance of the formed solid electrolyte interphase, shown in Figure 4b. Severely high interfacial resistances of 380 and 315 Ω, respectively, were found with electrolyte containing MeIm and DMA, matching the behavior observed during galvanostatic cycling. Cells with DMSO exhibited slightly smaller interfacial resistances of 70 Ω, while cells containing DME displayed relatively little impedance at all, on the order of 30 Ω. As cells with MeIm and DMA exhibited impedances an order of magnitude larger than those with DME, there is a clear need to understand the mechanism behind this severe instability.

The chemical stability of each solvent in contact with lithium metal was further investigated via $^1$H-nuclear magnetic resonance (NMR) spectroscopy. Solvents were placed in vials containing lithium metal, and were allowed to sit in static contact for approximately a week, before being assessed (as seen in Figure S3). As shown in Figure 5, after a week-long lithium-metal exposure, DMA, DMSO, and MeIm solvents display varying degrees of instability compared to the baseline scans performed with pristine solvent (shown in Figure

S4 **and** S5). No new peaks appear in the spectra of DMSO solvent, indicating that the solvent's instability with lithium metal likely results in the formation of an insoluble SEI product not detectable through sampling of the bulk solution. This may be in the form of cleavage of the DMSO molecule by lithium metal, which is expected to form lithium methanesulfenate by a mechanism suggested in a previous report.[30]

DMA solvent, however, shows evidence of considerable instability with lithium metal, with a disconcerting number of new peaks appearing over the entire range. The occurrence of new peaks at 4.53, 2.22, 2.13, 1.6, 1.1, and 0.9 ppm indicate a severe instability of DMA in contact with lithium. DMA has been reported to form dimethylamine in contact with lithium metal, suggesting particular instability with the central C-N single bond.[31] Dimethylamine exists in the gas phase at room temperature, which may account for the relative decrease in intensity of the peak at 2.95 ppm, and the resultant byproducts may account for the preponderance of new peaks that appear (see Figure S6 for more details). MeIm solvent displays the largest degree of instability with lithium metal among all of the evaluated solvents, with the emergence of several new peaks as well as the absence of an expected peak at 7.6 ppm. The complete absence of this peak clearly shows severe reaction with lithium metal has consumed the entire amount of MeIm reactant, and it suggests that the presence of the C-N single bond may serve as a common point of lithium metal instability with DMA. In the case of MeIm, a reaction occurring at this point could possibly open the imidazole ring, driving further side reactions and forming a multitude of decomposition products.[32] Further studies will likely be needed to confirm these hypotheses and have a more detailed understanding of the reactivity of these solvents with lithium metal. While all of the solvents provide a framework for thinking about a highly solvating Li-S battery electrolyte, their instability with lithium metal will need to be overcome through robust passivation and engineering of the lithium-metal anode.

A variation of this experiment was also conducted to evaluate the stability of dissolved polysulfides in each solvent over the course of 30 days. In each solvent, 0.5 M of $Li_2S_6$ was dissolved and allowed to sit in contact for 30 days, after which each sample was assessed with $^1H$ NMR. In contrast to lithium metal, each of the solvents exhibit rather robust stability when exposed to dissolved $Li_2S_6$ over the course of approximately one month. Each of the attained spectra closely correlate to what is observed in baseline scans performed with pristine solvent, with no additional peaks occurring in the spectra besides known contaminants.[33] This signals that the applicability of the highly solvating electrolyte framework to polysulfide species is not intrinsically limited, and suggests that further improvements using this approach will likely have to focus on protecting the lithium-metal anode.

## 3. Conclusion

Here, we have investigated highly solvating electrolytes as a framework for overcoming the limitations posed by Li-S surface-based reaction pathways. At high sulfur loadings and low E/S ratios, increased solubility towards lithium polysulfide species can prolong the extent of solution-mediated discharge and enable the truly high specific energy promise of Li-S batteries. Additionally, high donor number solvents have been revealed to have several

interesting properties at these previously unexplored conditions. DMSO and MeIm solvents exhibit diminished presence of $S_3^{\bullet-}$ at concentrated polysulfide conditions, which has a demonstrably negative effect on their ability to promote enhanced sulfur utilization compared to DMA solvent that displays substantial presence of $S_3^{\bullet-}$. The differences in the speciation observed in these solvents beckon further investigation into the mechanism behind each solvent's stabilization of radical species, and why this discrepancy occurs seemingly independent to metrics like donor number and dielectric constant. Indeed, the ability to solvate a greater amount of polysulfide species and the preferential stabilization of $S_3^{\bullet-}$ are not completely dependent variables, though both seem to be bearers of increased solution-based utilization.

However, all of the high donor number electrolytes exhibited inherent instability and uncontrolled decomposition in contact with lithium metal, as evident through investigations with electrochemical techniques and NMR. In contrast, the robust stability of polysulfide species in each solvent does demonstrate that there is not an intrinsic incompatibility of these solvents with the sulfur cathode and offers avenues for future development. Implementation of a robust passivating protection layer on lithium-metal anode would be able to shield the undesirable reactions with these solvents, while additionally mitigating the loss of active material from the inevitable increased polysulfide shuttling in highly solvating electrolytes. Additionally regardless of the electrolyte solvent used, complete passivation may likely be required for commercial implementation of lithium-metal anode.[34] In future studies, these solvents could also be tested in full-cell platforms that utilize alternative anodes or remove the lithium-metal anode entirely.[7,8,35,36] Finally, future efforts could use the studies here as a basis for molecular engineering and design of solvents with desirable functional groups to mitigate instabilities in contact with lithium metal altogether. A highly specialized solvating electrolyte, in combination with efforts into the cathode and anode, could be a necessary key in achieving the full potential of Li-S batteries.

## 4. Experimental Section

### Materials:

Sulfur ($S_8$, 99.5+%, Acros Organics), carbon disulfide ($CS_2$, extra pure, 99.9%, Acros Organics), carbon nanotubes (CNT) "buckypaper" (20 GSM, NanoTechLabs, Inc), carbon nanofibers (CNF, PR-19-XT-HHT, Pyrograf), lithium bis(trifluoromethanesulfonimide) (LiTFSI, $LiN(CF_3SO_2)_2$, 99%, Acros Organics), 1,2-dimethoxyethane (DME, 99+%, Acros Organics), 1,3-dioxolane (DOL, 99.5%, Acros Organics), N,N-dimethylacetamide (DMA, 99%, Sigma-Aldrich), dimethyl sulfoxide (DMSO, 99.9+%, Sigma-Aldrich), 1-methylimidazole (MeIm, 99+%, Sigma-Aldrich), metallic lithium foil (Aldrich Chemistry), PVDF Membrane Filter (0.1 μm, Durapore), lithium sulfide ($Li_2S$, 99.98%, Aldrich Chemistry), dimethyl sulfoxide-$d_6$ ($D_6$-DMSO, 99.9%, Acros Organics), and chloroform-d ($CDCl_3$, 99.8 atom % D, Acros Organics) were purchased and used as received.

### Sulfur-CNT Composite Cathode Fabrication:

Cathodes with 2 mg $cm^{-2}$ sulfur loading were fabricated by dissolving elemental sulfur in $CS_2$ at a mass ratio of 0.1 mg $\mu L^{-1}$, after which 20 μL of this solution was deposited onto a 1

$cm^2$ area CNT "buckypaper". This followed by slow drying overnight, yielding sulfur-CNT composite cathodes with an areal loading of 2.0 ± 0.15 mg $cm^{-2}$. 6 mg $cm^{-2}$ cathodes were fabricated by vacuum filtering a sonicated mixture of sulfur and CNF (3:1 m/m) in ethanol and water (1:1 v/v) onto a filter paper. The freestanding cathode membrane was peeled off and dried before being punched into 1 $cm^2$ electrode discs having an areal loading of 6.0 ± 0.2 mg $cm^{-2}$. CNF was used as it provided a more robust membrane.

### Electrolyte preparation:

Four electrolytes were prepared in an argon-filled glovebox by dissolving 1 M LiTFSI in a (1:1 v/v) mixture of DOL and DME, DOL and DMA, DOL and DMSO, and DOL and MeIm. $LiNO_3$, a standard Li-S electrolyte additive, was not used to allow for full assessment of active material utilization down to 1.5 V during discharge.

### Coin-cell Fabrication:

CR-2032 type coin cells were used for all electrochemical tests. lithium-sulfur half-cells with 2 mg $cm^{-2}$ sulfur loading were assembled inside an argon-filled glove box and utilized a sulfur-CNT composite cathode, a lithium metal foil anode, 40 μL of electrolyte (E/S = 20), and a ¾" diameter separator that was punched from a PVDF membrane filter. Half-cells were allowed to rest for 0.5 to 2 hours before beginning discharge to allow for a complete wetting of active material while minimizing lithium exposure to solvent pre-cycling. lithium-sulfur half-cells with 6 mg $cm^{-2}$ sulfur loading were assembled following the same procedure, except with 60 μL of electrolyte (E/S = 10). In symmetric cell studies, coin cells were assembled with lithium-metal-foil electrodes on both sides of the coin cell and 40 μL of electrolyte. At least 4 cells were made in each electrolyte to verify values attained and for replicability purposes (in both symmetric cells and lower-loading and high-loading half cells).

### Electrochemical Cell Testing:

An Arbin battery cycler was used to galvanostatically discharge cells at a *C* rate of C/10, corresponding to 0.334 mA. The cells were discharged to 1.5 V to fully assess material utilization and due to the absence of $LiNO_3$ additive in the electrolyte, which would normally decompose at such voltages. Cells were discharged to 1.4 V in the case of the .6 mg $cm^{-2}$ cells due to the high overpotentials. A BioLogic VMP2 potentiostat was used for electrochemical impedance spectroscopy (EIS) measurements with a scan range of $10^6$ Hz to $10^{-1}$ Hz and a 5 mV amplitude perturbation.

### Polysulfide Solution Preparation:

Polysulfide solutions samples were prepared by mixing an appropriate amount of $Li_2S$ and sulfur powder in each solvent such that the stoichiometric ratio of lithium and sulfur in solution was equivalent to $Li_2S_6$. First, 1.5 M nominal $Li_2S_6$ was prepared in 4 vials containing 3 mL of either DOL-DME (1:1 v/v), DMA, DMSO, or MeIm. This was done by adding 0.7215 g of elemental sulfur powder and 0.2067 g of $Li_2S$ powder into each vial, and then stirring each sample and heating to 60 ˚C such that all species dissolve. This high concentration solution was then diluted to make the 0.25 M $Li_2S_6$ samples that UV-Vis was

performed on. As 1.5 M $Li_2S_6$ is not soluble in DOL-DME at room temperature, this solution was heated to 60 ˚C such that all species were dissolved, and then immediately a sample was taken from this and diluted to make the lower concentration samples.

### Ultraviolet-Visible (UV-Vis) Spectrophotometry:

Polysulfide samples were diluted to 0.25 M and 0.01 M. In an argon-filled glovebox, 8 μL of each of these solutions were placed on the interior blank side of a 0.01 mm demountable short-path-length cuvette (White Bear Photonics, LLC), and then the corresponding exterior side was placed on top of it. This served to seal the sample well and to ensure it conformed to the 0.01 mm path length, both necessary conditions due to the opacity and air sensitivity of the liquid polysulfide samples. Each cuvette was then placed in a short-path-length cell holder (White Bear Photonics) which allowed for the use of each thin cuvette in a standard UV-Vis instrument sample chamber. A Cary 5000 UV-VIS NIR Spectrometer was used to characterize the samples from a wavelength range of 200 to 800 nm. The machine was operated in a single beam configuration, and baseline corrections were performed beforehand with a blank sample of each solvent.

### $^1$H-Nuclear Magnetic Resonance (NMR) Spectroscopy:

1 mL of each solvent sample was placed in a vial that had a 3/8” diameter lithium chip placed at its base. Solvents sat in static equilibrium in contact with the lithium metal for 7 days, and then 10 μL of each solvent was drawn from each vial and placed in an NMR tube with 700 μL of $CDCl_3$, or $D_6$-DMSO in the case of DMA and MeIm. Additionally, 0.5 M $Li_2S_6$ was dissolved in separate vials of each solvent and allowed to sit at static equilibrium for 30 days, after which 10 μL of each sample was placed in a NMR tube with 700 μL $D_6$-DMSO. $^1$H-NMR spectroscopy was performed via a Bruker Avance III 500 MHz NMR spectrometer. 32 scans of each sample were performed, and the chemical shifts (δ) were calibrated using the residual solvent peak as an internal standard.

## Supplementary Material

Refer to Web version on PubMed Central for supplementary material.

## Acknowledgements

Financial support through a NASA Space Technology Research Fellowship under award number 80NSSC17K0089 is gratefully acknowledged. Additionally, helpful and informative discussions with Drs. Ratnakumar Bugga and John-Paul Jones are gratefully acknowledged.

## References

[1]. Manthiram A, Chung S-H, Zu C, Adv. Mater 2015, 27, 1980. [PubMed: 25688969]

[2]. Hong-Jie P, Jia-Qi H, Xin-Bing C, Qiang Z, Adv. Energy Mater 2017, 7, 1700260.

[3]. Chung S-H, Chang C-H, Manthiram A, Adv. Funct. Mater 2018, 28, 1801188.

[4]. Mikhaylik YV, Akridge JR, J. Electrochem. Soc 2003, 150, A306.

[5]. Cuisinier M, Hart C, Balasubramanian M, Garsuch A, Nazar LF, Adv. Energy Mater 2015, 5, 1401801.

[6]. Son Y, Lee J-S, Son Y, Jang J-H, Cho J, Adv. Energy Mater 2015, 5, 1500110.

[7]. Zhang K, Wang L, Hu Z, Cheng F, Chen J, Sci. Rep 2015, 4, 6467.

[8]. Thieme S, Brückner J, Meier A, Bauer I, Gruber K, Kaspar J, Helmer A, Althues H, Schmuck M, Kaskel S, J. Mater. Chem. A 2015, 3, 3808.

[9]. Agostini M, Xiong S, Matic A, Hassoun J, Chem. Mater 2015, 27, 4604.

[10]. Li W, Yao H, Yan K, Zheng G, Liang Z, Chiang Y-M, Cui Y, Nat. Commun 2015, 6, 7436. [PubMed: 26081242]

[11]. Shen C, Xie J, Zhang M, Andrei P, Hendrickson M, Plichta EJ, Zheng JP, Electrochim. Acta 2017, 248, 90.

[12]. McCloskey BD, J. Phys. Chem. Lett 2015, 6, 4581. [PubMed: 26722800]

[13]. Qie L, Zu C, Manthiram A, Adv. Energy Mater 2016, 6, 1502459.

[14]. Hagen M, Hanselmann D, Ahlbrecht K, Maça R, Gerber D, Tübke J, Adv. Energy Mater 2015, 5, 1401986.

[15]. Cuisinier M, Cabelguen P-E, Adams BD, Garsuch A, Balasubramanian M, Nazar LF, Energy Environ. Sci 2014, 7, 2697.

[16]. Lee C-W, Pang Q, Ha S, Cheng L, Han S-D, Zavadil KR, Gallagher KG, Nazar LF, Balasubramanian M, ACS Cent. Sci 2017, 3, 605. [PubMed: 28691072]

[17]. Suo L, Hu Y-S, Li H, Armand M, Chen L, Nat. Commun 2013, 4, 1481. [PubMed: 23403582]

[18]. Johnson L, Li C, Liu Z, Chen Y, Freunberger SA, Ashok PC, Praveen BB, Dholakia K, Tarascon J-M, Bruce PG, Nat. Chem 2014, 6, 1091. [PubMed: 25411888]

[19]. Zou Q, Lu Y-C, J. Phys. Chem. Lett 2016, 7, 1518. [PubMed: 27050386]

[20]. Bonnaterre R, Cauquis G, J. Chem. Soc. Chem. Commun 1972, 0, 293.

[21]. Liu J, Jia G, Colloid Polym. Sci 2015, 293, 2053.

[22]. Chivers T, Elder PJW, Chem. Soc. Rev 2013, 42, 5996. [PubMed: 23628896]

[23]. Wujcik KH, Wang DR, Raghunathan A, Drake M, Pascal TA, Prendergast D, Balsara NP, J. Phys. Chem. C 2016, 120, 18403.

[24]. Wujcik KH, Pascal TA, Pemmaraju CD, Devaux D, Stolte WC, Balsara NP, Prendergast D, Adv. Energy Mater 2015, 5, 1500285.

[25]. Barchasz C, Molton F, Duboc C, Leprêtre J-C, Patoux S, Alloin F, Anal. Chem 2012, 84, 3973. [PubMed: 22482872]

[26]. Kim B-S, Park S, J. Electrochem. Soc 1993, 140, 115.

[27]. Martin RP, Doub WH, Roberts JL, Sawyer DT, Inorg. Chem 1973, 12, 1921.

[28]. Scheers J, Fantini S, Johansson P, J. Power Sources 2014, 255, 204.

[29]. Peled E, Sternberg Y, Gorenshtein A, Lavi Y, J. Electrochem. Soc 1989, 136, 1621.

[30]. Brandsma L, Meijer J, Verkruijsse HD, Recl. des Trav. Chim. des Pays-Bas 1976, 95, 79.

[31]. Uddin J, Bryantsev VS, Giordani V, Walker W, Chase GV, Addison D, J. Phys. Chem. Lett 2013, 4, 3760.

[32]. Carver CT, Diaconescu PL, J. Am. Chem. Soc 2008, 130, 7558. [PubMed: 18491906]

[33]. Fulmer GR, Miller AJM, Sherden NH, Gottlieb HE, Nudelman A, Stoltz BM, Bercaw JE, Goldberg KI, Organometallics 2010, 29, 2176.

[34]. Chen Y, Freunberger SA, Peng Z, Bardé F, Bruce PG, J. Am. Chem. Soc 2012, 134, 7952. [PubMed: 22515410]

[35]. Brückner J, Thieme S, Böttger-Hiller F, Bauer I, Grossmann HT, Strubel P, Althues H, Spange S, Kaskel S, Adv. Funct. Mater 2014, 24, 1284.

[36]. Nanda S, Gupta A, Manthiram A, Adv. Energy Mater 2018, 8, 1801556.

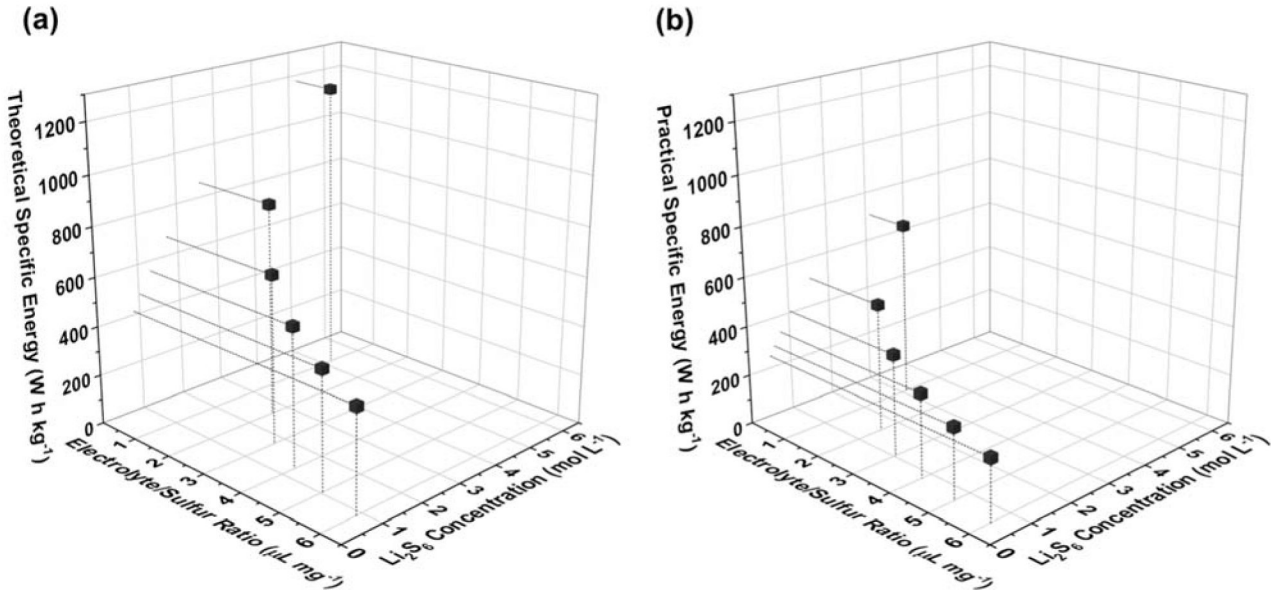


**Figure 1.**

Graphical representation of the interplay between specific energy, electrolyte-to-sulfur ratio, and required concentration of polysulfide species if (a) a capacity of 1,672 m Ah $g^{-1}$ or (b) a capacity of 1,000 m Ah $g^{-1}$ is attained at the active material level.

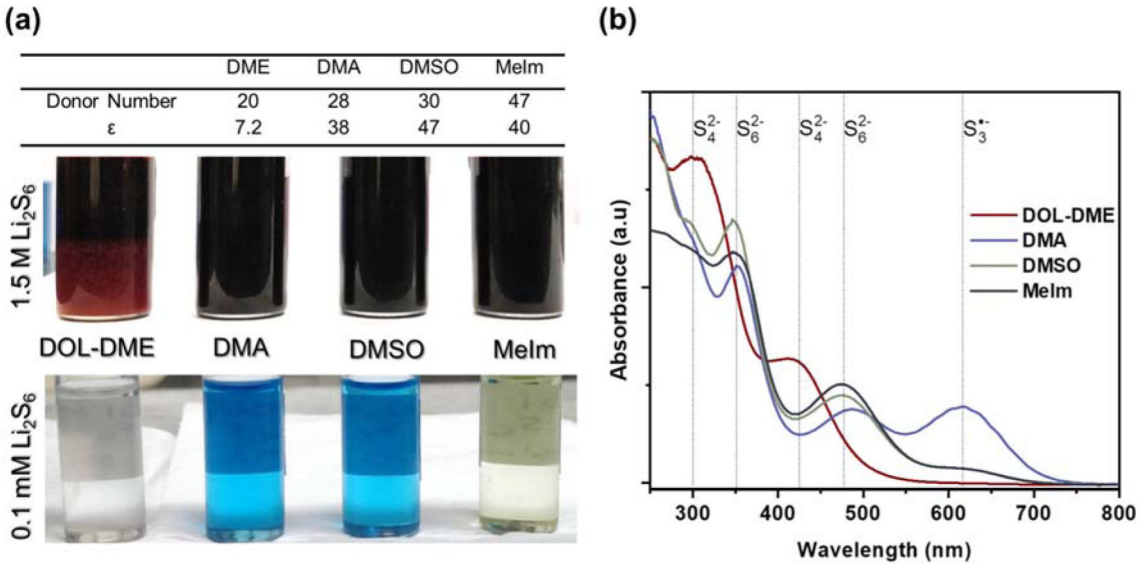


**Figure 2.**

(a) Donor number and dielectric constant (ε) of the different solvents investigated, along with optical images of vials containing 1.5 M and 0.1 mM nominal $Li_2S_6$ dissolved in each solvent. A clear blue color, indicative of the $S_3^{\bullet-}$ radical species, is predominant in DMA and DMSO at low concentrations.[5,15,16,18,19] (b) UV-Vis spectra obtained for 0.25 M nominal $Li_2S_6$ (1.5 M of Sulfur) in DOL-DME, DMA, DMSO, and MeIm, with associated peak identification. [16,17,22-24]

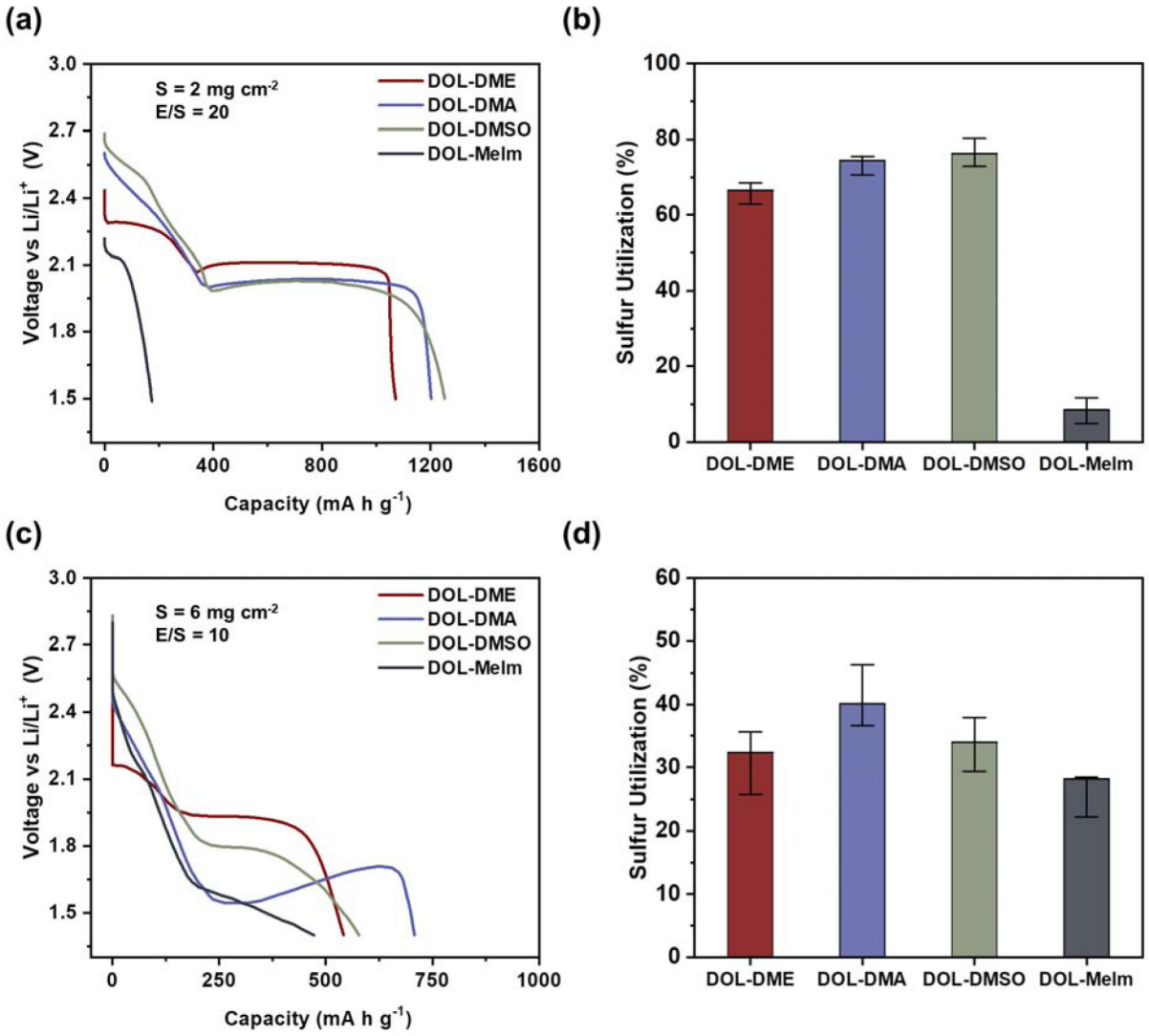


**Figure 3.**

(a) First cycle discharge profiles of 2 mg $cm^{-2}$ sulfur cathode obtained for a sulfur cathode in 4 different electrolytes, where the solvents of interest are used with 50% DOL and 1 M LiTFSI. (b) Bar graph showing median utilizations obtained at 2 mg $cm^{-2}$, along with the range of values observed. (c) First cycle discharge profiles of 6 mg $cm^{-2}$ sulfur cathode. (d) Median utilizations obtained for 6 mg $cm^{-2}$ cathodes, along with the range of values observed.

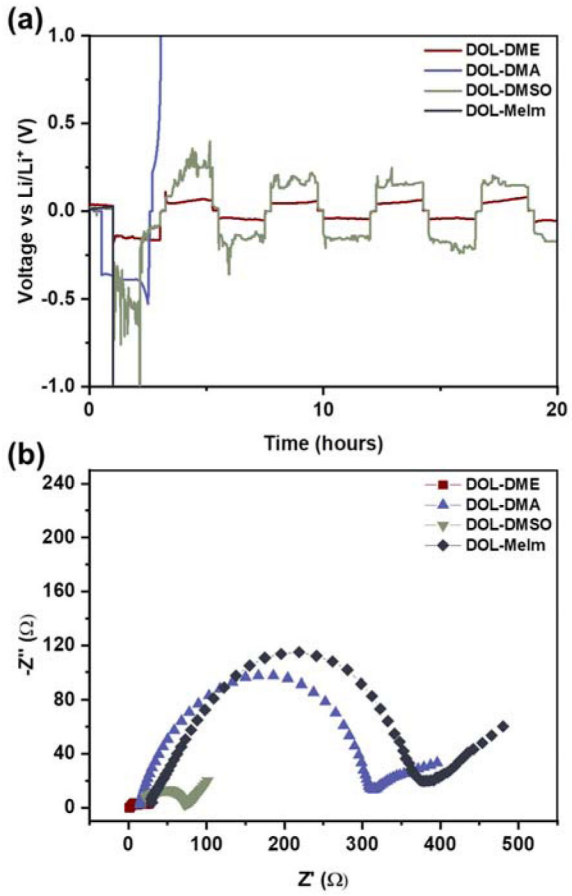


**Figure 4.**

(a) Galvanostatic cycling of lithium symmetric cells in DOL-DME, DOL-DMA, DOL-DMSO, and DOL-MeIm electrolytes. (b) Electrochemical impedance spectra of each cell after a single lithium plating and stripping cycle, or after failure in the case of DOL-DMA and DOL-MeIm.

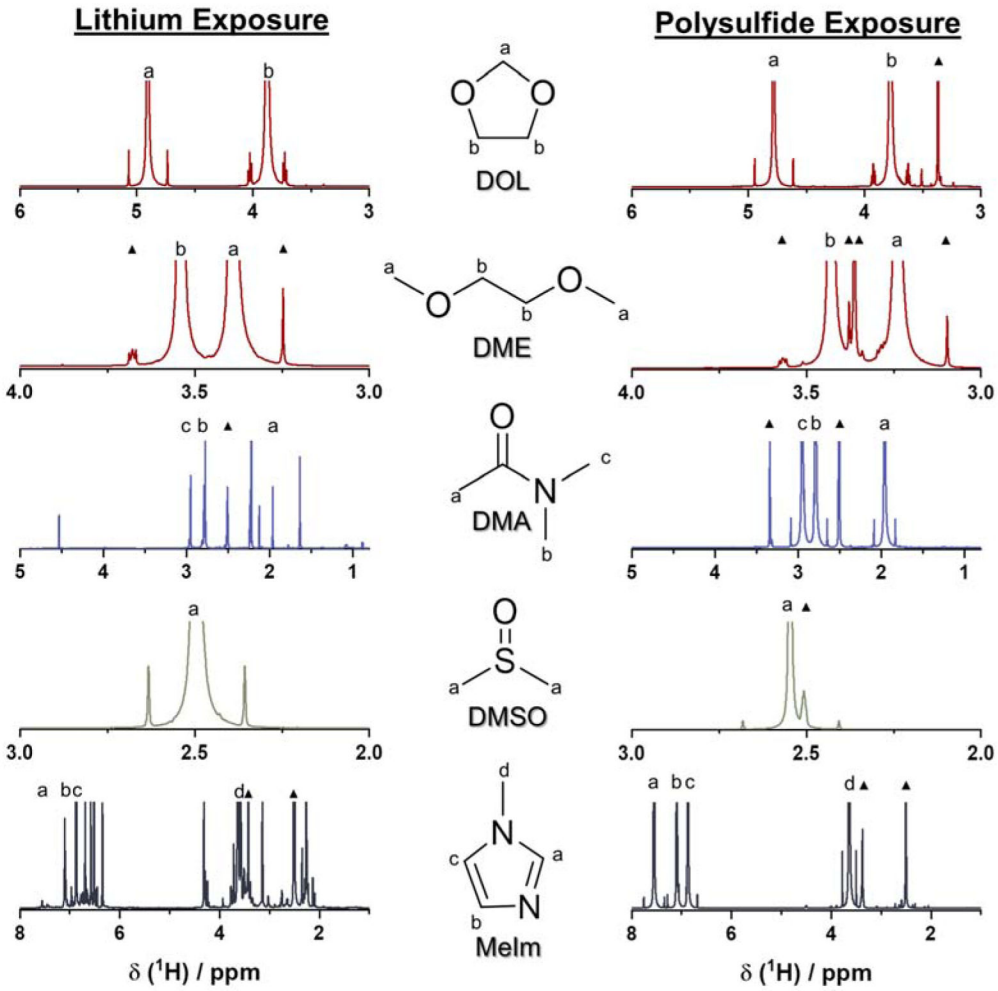


**Figure 5.**

$^{1}$H-NMR spectra of each of the solvents under investigation after exposure to lithium metal for one week (left) and dissolved polysulfides for 30 days (right). Hydrogens associated with each peak are labelled on each solvent molecule as well as on the spectra themselves. Unlabeled peaks correspond to suspected decomposition products. The symbol "▲" accompanies peaks corresponding to known contaminants, unaffiliated with suspected side reactions. [33]